

Porous coordination polymers constructed from anisotropic metal–carboxylate–pyridyl clusters*

Yue-Biao Zhang and Jie-Peng Zhang[‡]

MOE Key Laboratory of Bioinorganic and Synthetic Chemistry, School of Chemistry and Chemical Engineering, Sun Yat-Sen University, Guangzhou 510275, China

Abstract: While isotropic metal–carboxylate clusters as secondary building blocks have enabled the rational design of porous coordination polymers (PCPs) with predictable topologies, augmented metal–carboxylate–pyridyl clusters can be used as anisotropic secondary building blocks to facilitate the construction of higher-connectivity frameworks and control over structural directionality in self-assembly.

Keywords: coordination polymers; crystal engineering; metal–organic frameworks; porous materials; reticular chemistry.

INTRODUCTION

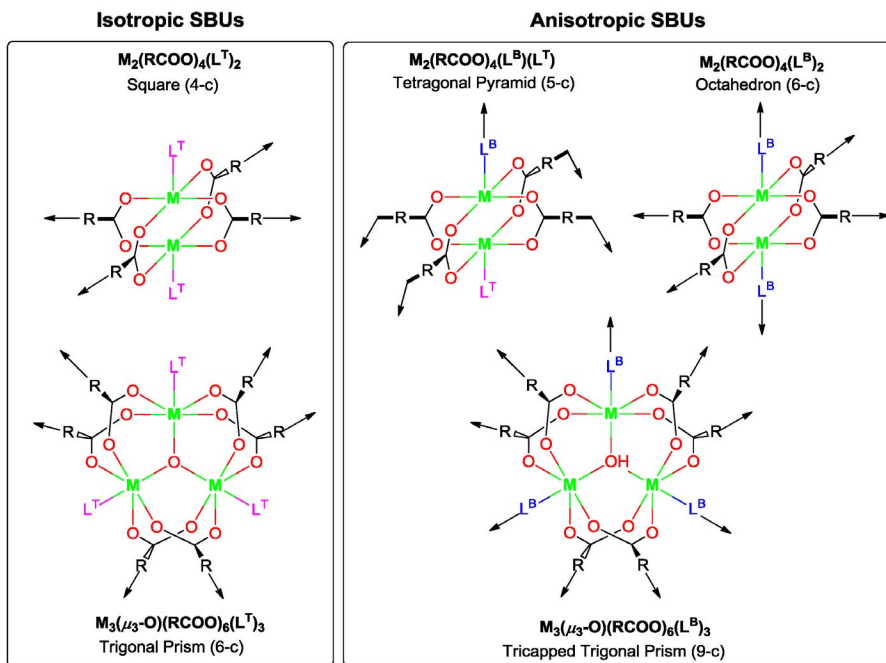
Porous coordination polymers (PCPs), also known as metal–organic frameworks (MOFs) [1], are periodic networks composed of metal ions (or clusters) and organic ligands. These crystalline materials can possess diverse framework structures and functionalities, which are promising for future clean energy and environment applications [2,3]. Although the past two decades have witnessed the great development of PCPs, rational design of new structural types remains a great challenge.

Crystal engineering of PCPs mainly depends on the judicious selection or design of organic ligands. Up to date, the most-used organic ligands are mainly based on *N*- and *O*-donor functionalities, which show different coordination behaviors. Each *N*-donor in pyridyl, nitrile, amine, or azole group usually binds only one transition-metal ions, which facilitate the predetermination of local coordination structures. However, the coordination bonds between transition-metal ions and these neutral ligands are generally weak, and the metal–ligand ratios are difficult to be controlled, which ultimately puzzle the resulting structures. Recently, azolate anions such as imidazolate and triazolate derivatives have been proven as very versatile ligands for construction of highly robust PCPs [4]. The most familiar *O*-donor coordination group is carboxylate, which is electronegative with relatively strong binding ability to transition-metal ions. Because carboxylate possesses variable coordination modes (such as chelating, bridging, and chelating–bridging), some robust metal–carboxylate clusters with well-defined geometries are usually used as building blocks to facilitate structure prediction and design. The $M_2(RCOO_2)(L^T)_2$ (L^T = terminal ligand), $M_4(\mu_4-O)(RCOO)_6$, $M_3(\mu_3-O/OH)(RCOO)_6(L^T)_3$ clusters have been widely used as isotropic building blocks (or secondary building units, SBUs) with 4-connected square, 6-connected octahedron, and 6-connected trigonal-prism geometries, respectively.

*Pure Appl. Chem. **85**, 315–462 (2013). A collection of invited papers based on presentations at the 12th Eurasia Conference on Chemical Sciences, Corfu, Greece, 16–21 April 2012.

[‡]Corresponding author: E-mail: zhangjp7@mail.sysu.edu.cn

The knowledge of periodic networks or topologies can facilitate not only the understanding, description, and classification of existing frameworks, but also the conceiving of new PCPs. The systematic enumeration of periodic networks has established several comprehensive topology libraries, such as the Reticular Chemistry Structure Resource (RCSR; nets are symbolized as bold, lowercase, three-letter codes) [5]. In the net-based approach or reticular chemistry, the most accessible prototypes are simple and high-symmetry topologies, because they significantly reduce the almost infinite number of possibilities [6]. The simplest topologies are uninodal, comprising only one kind of node and one kind of edge, which can be mimicked by one kind of metal ions and one kind of ligand. For examples, the 4-connected **nbo**, 6-connected **pcu**, 6-connected **acs**, and 12-connected **fcu** nets can be constructed by linking the square $M_2(RCOO)_4(L^T)_2$ [7], octahedral $M_4(\mu_4-O)(RCOO)_6$ [8], trigonal-prismatic $M_3(\mu_3-O/OH)(RCOO)_6(L^T)_3$ [9], and cuboctahedral $Zr_6(\mu_4-O)_4(OH)_4(RCOO)_{12}$ [10] clusters, respectively, with dicarboxylate ligands. In these binary metal–ligand systems, the pore sizes can be controlled by the lengths of linkers, but the pore shapes are unalterable. To change the pore size and shape simultaneously, a higher level of structure complexity should be necessary. The first strategy is to use mixed ligands. For example, the isotropic $Zn_4(\mu_4-O)(RCOO)_6$ cluster can be connected by mixed dicarboxylate/tricarboxylate linkers to form complicated ternary metal–ligand systems, giving very different topologies when changing the length ratio of linkers [11–15]. Another strategy is to use intrinsic ternary metal–ligand systems, such as those composed of anisotropic clusters (two kinds of coordination functionalities) and two kinds of linkers. Actually, these anisotropic clusters are widely encountered in PCPs. As shown in Scheme 1, the $M_2(RCOO)_4(L^T)_2$ and $M_3(\mu_3-O/OH)(RCOO)_6(L^T)_3$ clusters are usually used as isotropic 4- and 6-connected nodes when only the carboxylate functionalities are substituted. However, when the terminal site is also substituted by a bridging ligand (L^B) these clusters become anisotropic building blocks with higher connectivity, which have been used to construct many interesting PCPs.



Scheme 1 Some typical metal–carboxylate clusters as isotropic and anisotropic SBUs.

USING $M_2(RCOO)_4(L^B)(L^T)$ CLUSTERS AS 5-CONNECTED NODES

When the four carboxylate sites of the $M_2(RCOO)_4(L^T)_2$ cluster are extended and bended toward one side, the two terminal sites can be substituted only on the opposite side, giving $M_2(RCOO)_4(L^B)(L^T)$ as a 5-connected square-pyramidal building block. The most typical structures composed of the $M_2(RCOO)_4(L^T)_2$ with bend dicarboxylates are the high-symmetric metal-organic polyhedrons (MOPs) $[M_{24}(ip)_{24}(L^T)_{24}]$ (ip^{2-} = isophthalate derivatives), which is a cuboctahedral cage composed of 12 paddle-wheel clusters and 24 ditopic linkers with 120° bend. The 24 terminal ligands coordinated at the dinuclear cluster point to two different orientations: 12 towards the center of the cage, and the other 12 outwards from the cage. Obviously, the inner terminal ligands confined by the cage cannot be used as extension sites. Nevertheless, using the 12 outward terminal sites, the MOP can serve as a 12-connected cuboctahedral building block (Fig. 1c), which is ideal for the construction of the face-centered cubic net (**fcu**, Fig. 1a). Considering the $M_2(RCOO)_4(L^B)(L^T)$ clusters as nodes, the network can be described as the uninodal 5-connected **ubt** net (Fig. 1b) or the augmented **fcu** (**fcu-a**) net. The uninodal 5-connected **ubt** net consists of three kinds of tiles described as $2[3^4 \cdot 6^4] + [3^8 \cdot 4^6] + [4^6 \cdot 6^8]$. That is, three polyhedral cages, including cuboctahedron, truncated tetrahedron, and truncated octahedron in the ratio of 2:1:1.

Chun et al. mixed Zn^{2+} , 5-methylisophthalic acid (H_2mip), and 1,4-diazabicyclo-[2.2.2]octane (dabco) in a one-pot solvothermal reaction to obtain the first **ubt**-type framework $[Zn_{24}(mip)_{24}(dabco)_6(H_2O)_{12}]$ [16]. This structure contains a hierarchical pore system consisting of cuboctahedron, truncated tetrahedron, and truncated octahedron cages as defined by the topology, with pore diameters of 12, 9, and 17 Å, respectively, and Langmuir surface area more than 2000 m²/g. They further showed that **ubt**-type frameworks can be also constructed by ip^{2-} and Zn^{2+}/Co^{2+} , as well as a longer linker naphthalene-2,7-dicarboxylate ($2,7-ndc^{2-}$, Fig. 1d) [17]. Wang and Su et al. also used 5-aminoisophthalate (aip^{2-}) and 4,4'-bipyridine (bpy) with Cu^{2+} to obtain a **ubt**-type framework $[Cu_{24}(aip)_{24}(bpy)_6(H_2O)_{12}]$ (Fig. 1e) with pore diameters of 12, 15, and 24 Å, which demonstrated promising property for drug delivery [18]. Obviously, this ternary metal-ligand system shows the

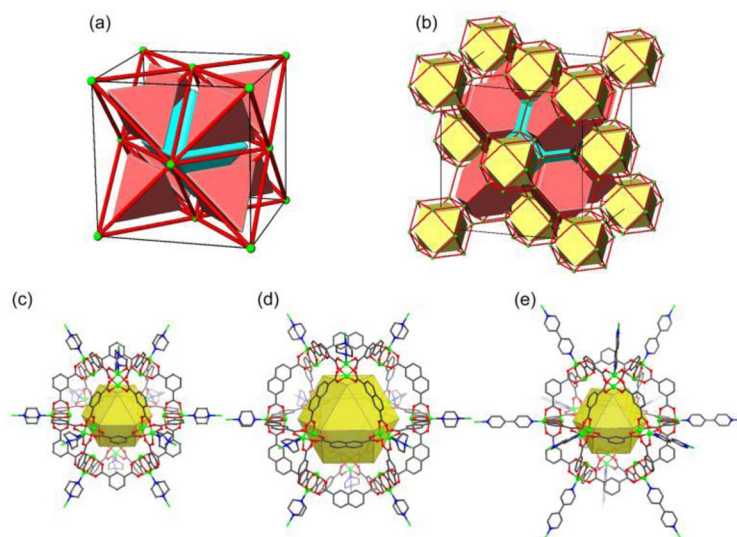


Fig. 1 Constructing 3D PCPs with the **ubt** (**fcu-a**) topology using 5-connected $M_2(RCOO)_4(L^B)(L^T)$ clusters: (a) The net and tiling presentation of **fcu**; (b) the net and tiling presentation of **ubt** (**fcu-a**); (c) extending the cuboctahedral MOP $[M_{24}(ip)_{24}]$ with 12 dabco linkers; (d) extending the cuboctahedral MOP $[M_{24}(2,7-ndc)_{24}]$ with 12 dabco linkers; (e) extending the cuboctahedral MOP $[M_{24}(aip)_{24}]$ with 12 bpy linkers (amino groups on aip^{2-} are omitted for clarity).

ability of anisotropic modification of pore sizes by lengthening either the dicarboxylate or the bpy-like ligand without altering the **ubt** topology.

Another typical type of MOP is an octahedral cage constructed by 6 $M_2(RCOO)_4(L^T)_2$ clusters and 12 dicarboxylates with a 90° bend, which was firstly designed by Yaghi et al. by using 2,2':5',2''-terthiophene-5,5''-dicarboxylate [19]. The six exterior terminal ligands can be substituted to construct a primitive cubic array (**pcu**, Fig. 2a) of octahedral MOPs, which can be also simplified as the uninodal 5-connected **cab** (CaB_6 , Fig. 2b) or **pcu-a** net considering the dinuclear clusters as nodes (Fig. 2c). In 2011, Zhou et al. discovered another octahedral MOP $[Cu_{12}(cdc)_{12}(H_2O)_{12}]$ (Fig. 2c; $cdc^{2-} = 9H$ -carbazole-3,6-dicarboxylate) with the pore diameter of 14 Å. Further mixing the MOP solution with bpy, a 2-fold interpenetrating **cab** framework (Fig. 2d) was obtained, in which the truncated cubic cavities with pore diameter of ~30 Å were inhabited by octahedral cages from another identical set of **cab** frameworks [20]. Featuring the first case of step-wise construction of polyhedra-based framework, it was indicated that the framework is difficult to be obtained by the one-pot reaction. Furthermore, the framework can disassemble back into the isolate MOP after treating with pyridine (py).

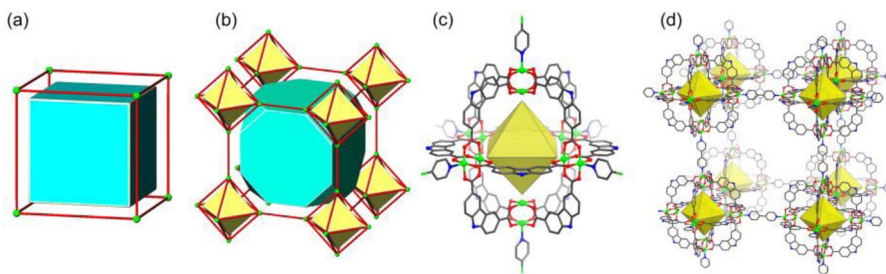


Fig. 2 Constructing 3D PCPs with the **cab** (**pcu-a**) topology using 5-connected $M_2(RCOO)_4(L^B)(L^T)$ clusters: (a) The net and tiling presentation of **pcu**; (b) the net and tiling presentation of **cab** (**pcu-a**); (c) structure of the octahedral MOP $[Cu_{12}(cdc)_{12}(py)_6]$; (d) a portion of the crystal structure of $[Cu_{12}(cdc)_{12}(bpy)_3]$.

USING $M_2(RCOO)_4(L^B)_2$ CLUSTERS AS 6-CONNECTED NODE

More commonly, $M_2(RCOO)_4(L^T)_2$ clusters can be augmented as asymmetric 6-connected $M_2(RCOO)_4(L^B)_2$, in which both terminal ligands are substituted by bridging ligands. Using linear dicarboxylates, the $M_2(RCOO)_4(L^T)_2$ clusters usually serve as 4-connected nodes to form square grid layers (**sql** net, Fig. 3a), which can be further pillared by bpy-like ligands into 3D frameworks with the **pcu** topology. Seki and Mori et al. proposed this strategy to construct a series of 3D frameworks by intercalating the 2D Cu^{II} /dicarboxylate frameworks with dabco as a pillared ligand, which demonstrated higher porosity and methane adsorption behaviors, albeit crystal structures for X-ray diffraction structure analysis were not obtained [21,22]. Later, Kim et al. reported the single-crystal structure and guest-dependent dynamic behavior of $[Zn_2(bdc)_2(dabco)]_n$ (Fig. 3b) synthesized by a one-pot solvothermal reaction [23]. With the short pillar-linker dabco, this prototype can be expanded without interpenetration by lengthening the dicarboxylates to expand the channel sizes (Fig. 3c) [24]. When lengthening the pillar-linker, such as to bpy, interpenetration usually occurred even with a shorter dicarboxylate such as fumarate [25]. Nevertheless, by introducing adequate steric hindrance on the dicarboxylate to block the apertures on the layers, non-interpenetrating frameworks (Fig. 3d) have been obtained with bpy as the pillar-linker [26,27]. In principle, this ternary metal–ligand prototype represents the abilities for systematic control of pore sizes/shapes, interpenetration and internal surface properties by modifying the lengths or functionality on either or both of the layer- and pillar-linkers, which can provide greater structural diversity and optimal adsorption properties.

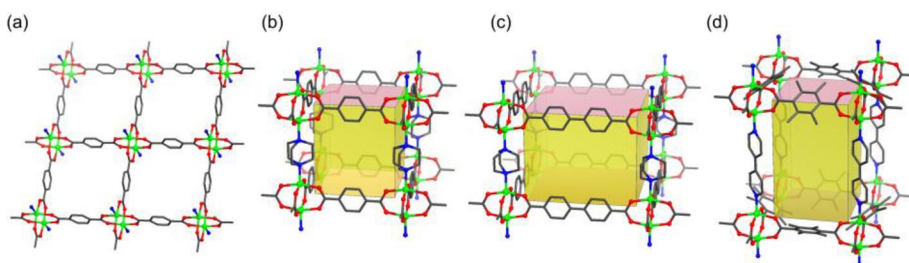


Fig. 3 From 2D grid layer (a) to 3D noninterpenetrated pillared grid-layer frameworks using the $M_2(RCOO)_4(L^B)_2$ clusters and different ligands (b, very short layer- and pillar-linkers; c, a long layer-linker and the shortest pillar-linker dabco; d, a long pillar-linker bpy and a layer-linker with large steric hindrance).

Framework isomerism is an interesting phenomenon in PCPs, which means that a given set of molecular building blocks can give more than one resultant framework structure [28]. Actually, the square grid layer is not the only target when linking the paddle-wheel cluster with the dicarboxylate linker. It is possible to obtain the Kagome layer by linking $M_2(RCOO)_4(L^T)_2$ clusters with dicarboxylates (Fig. 4a), which can be pillared by bpy-like ligands into 3D frameworks with the **kag** topology. By carefully modifying the synthetic condition, Chun and Moon synthesized the first pillared Kagome-layer framework $[Zn_2(bdc)_2(dabco)]_n$ (Fig. 4b) [29]. With the identical framework compositions to the pillared grid-layer one, the pillared Kagome-layer framework possesses higher porosity and larger channels. Further, Kitagawa et al. discovered that this pair of isomeric frameworks can be selectively synthesized by controlling the synthetic temperature [30]. They also synthesized another pillared Kagome-layer framework with a longer pillar ligand bpy (Fig. 4c), in which interpenetration is absent because **kag** is not self-dual as **pcu**.

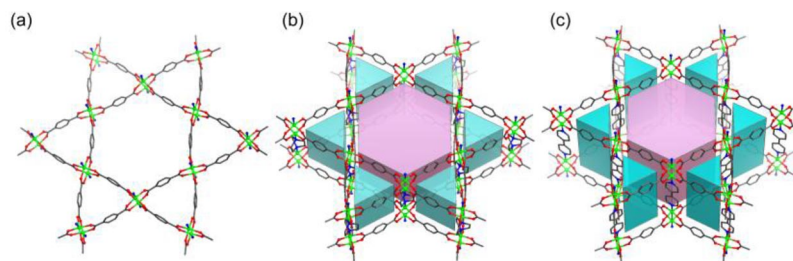


Fig. 4 From 2D Kagome layer (a) to 3D pillared Kagome-layer frameworks (b, dabco as pillar; c, bpy as pillar) using the $M_2(RCOO)_4(L^B)_2$ clusters.

Besides the combination of bipyridyl–dicarboxylate, mixing pyridyl–carboxylate and dicarboxylate in a ratio of 2:1 can also satisfy the 2:1 functionality ratio for the 6-connected $M_2(RCOO)_4(L^T)_2$ clusters. Zeng et al. firstly demonstrated that $Zn_2(RCOO)_4(L^T)_2$ can be connected by mixed ligands of isonicotinate and succinate–fumarate to form 2-fold interpenetrating 6-connected **pcu** nets (Fig. 5a) [35]. Recently, by extending both of the linkers, a porous doubly interpenetrating framework $[Zn_2(pba)_2(bdc)]_n$ [$pba^- = 4\text{-(pyridin-4-yl)benzoate}$] was reported by Chen et al. (Fig. 5b) [36]. Although it seems more difficult to control over the interpenetration, this strategy can provide an alternative prototype for constructing porous interpenetrating frameworks with the potential application of separation comparable to the interpenetrating pillared grid-layer frameworks.

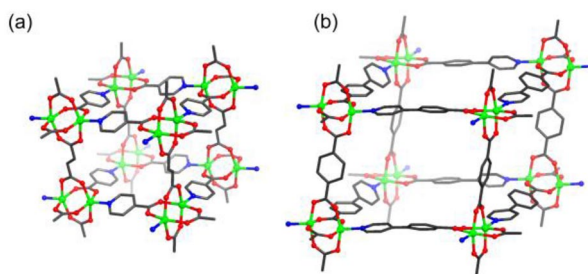


Fig. 5 The mixed pyridyl–carboxylate–dicarboxylate ligand strategy for constructing **pcu**-type frameworks based on $\text{Zn}_2(\text{RCOO})_4(\text{L}^{\text{B}})_2$ clusters.

Besides the combination of two types of ditopic linkers, the 2:1 functionality ratio of the 6-connected $\text{M}_2(\text{RCOO})_4(\text{L}^{\text{B}})_2$ cluster can also be met by a single tripodal ligand with one pyridyl and two carboxylate groups. Recently, Eddaoudi et al. constructed a series of PCPs by linking the paddle-wheel $\text{Cu}_2(\text{RCOO})_4(\text{L}^{\text{B}})_2$ cluster with 5-(4*H*-1,2,4-triazol-4-yl)isophthalate, 5-(pyridin-4-ylmethoxy)isophthalate, 5-(pyridin-3-ylmethoxy)isophthalate, and (*E*)-5-{[4-(benzyloxy)phenyl]diazanyl}isophthalate [33]. A pair of isomeric frameworks has been isolated with 5-(pyridin-4-ylmethoxy)isophthalate (Fig. 6), which can be described as pillared grid-layer and pillared Kagome-layer frameworks considering the metal–carboxylate networks as layers and the pyridyl ends as pillars. The pillared grid-layer structure can be formally described as a binodal (3,6)-connected **rtl** topology regarding the ligand as 3-connected and the $\text{M}_2(\text{RCOO})_4(\text{L}^{\text{B}})_2$ cluster as 6-connected nodes. Similar porous frameworks have also been reported by Zhang et al., in which $\text{Cu}_2(\text{RCOO})_4(\text{L}^{\text{B}})_2$ clusters were linked by 5-(pyridin-4-yl)isophthalate and 5-(pyridin-3-yl)isophthalate [34].

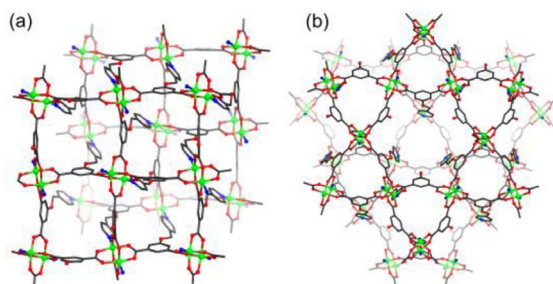


Fig. 6 Isomeric pillared grid-layer (a) and pillared Kagome-layer (b) (3,6)-connected frameworks constructed by 6-connected $\text{Cu}_2(\text{RCOO})_4(\text{L}^{\text{B}})_2$ clusters and a tripodal ligand 5-(pyridin-4-ylmethoxy)isophthalate.

USING $\text{M}_3(\text{RCOO})_6(\text{L}^{\text{B}})_3$ AS 9-CONNECTED NODE

As another typical type of metal–carboxylate clusters, $\text{M}_3(\mu_3\text{-O/OH})(\text{RCOO})_6(\text{L}^{\text{T}})_3$ performed as isotropic, 6-connected SBUs with trigonal-prism geometry in the construction of PCPs, which are known as MIL-101 series with the **mtm-e** topology [37] and MIL-88 series with the **acs** topology [38]. In these frameworks, the terminal sites are generally occupied by counter anions or solvent molecules. When the three terminal sites on $\text{M}_3(\mu_3\text{-O/OH})(\text{RCOO})_6(\text{L}^{\text{T}})_3$ are entirely substituted by bridging ligands, the cluster become anisotropic 9-connected SBUs with tricapped-trigonal-prism geometry, which in principle requires a 2:1 molar ratio of carboxylate and pyridyl groups, either from one type of ligand or from mixed ligands.

Obviously, a ditopic linker can never fulfill the requirement of 2:1 ratio of carboxylate and pyridyl. On the other hand, a tritopic linker with two carboxylates and one pyridyl group shows the prime feasibility, which is supposed to form binodal (3,9)-connected networks, as the linker serves as a 3-connected node. Zhang and Chen et al. firstly realized this strategy and constructed a new binodal (3,9)-connected (the topology was named as **xmz**, Fig. 7a) framework (Fig. 7b) by using pyridine-3,5-dicarboxylate (pdc^{2-}) and $\text{Co}_3(\mu_3\text{-OH})(\text{RCOO})_6(\text{L}^{\text{B}})_3$ [39]. By using 4,4'-(pyridine-3,5-diyl)dibenzate (pdb^{2-}) with a longer branch length, Schröder et al. reported two isorecticular porous frameworks based on $\text{Ni}_3(\mu_3\text{-OH})(\text{RCOO})_6(\text{L}^{\text{B}})_3$ and $\text{Fe}_3(\mu_3\text{-O})(\text{RCOO})_6(\text{L}^{\text{B}})_3$ clusters (Fig. 7c) in the mean time, though their topologies were described as a 12-connected net.

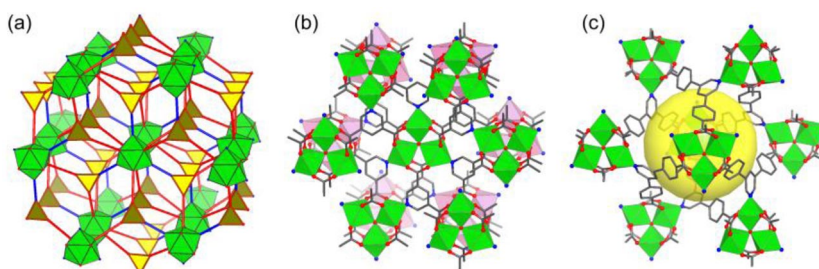


Fig. 7 The (3,9)-connected **xmz** topology (a) and two reported examples based on $\text{M}_3(\mu_3\text{-OH/O})(\text{RCOO})_6(\text{L}^{\text{B}})_3$ clusters and pdc^{2-} (b) or pdb^{2-} (c).

Rational combinations of two types of ditopic ligands may also furnish the functionality ratio requirement for the 9-connected $\text{M}_3(\mu_3\text{-O/OH})(\text{RCOO})_6(\text{L}^{\text{B}})_3$ clusters. For examples, mixing bipyridyl and dicarboxylates in 1:2 molar ratio, or pyridyl–carboxylate and dicarboxylates in 2:1 molar ratio can both satisfy the requirement, which might extend the $\text{M}_3(\mu_3\text{-O/OH})(\text{RCOO})_6(\text{L}^{\text{T}})_3$ clusters into uninodal 9-connected frameworks. After a comprehensive survey of possible uninodal 9-connected topologies, the **ncb** net was selected as the most promising target, because it is the simplest (one kind of node with two kinds of edges) with high-symmetry ($I-43m$) (Fig. 8a), and its node ($3m$, Fig. 8b) is also similar to the cluster in geometry (tricapped-trigonal-prism). In **ncb**, the three capped-vertices and six prismatic-vertices of the tricapped-trigonal-prismatic node are interconnected in two distinct fashions, capped-vertex to prismatic-vertex and prismatic-vertex to prismatic-vertex, in a 2:1 ratio (Fig. 8c). Therefore, employing the $\text{M}_3(\mu_3\text{-O/OH})(\text{RCOO})_6(\text{L}^{\text{B}})_3$ clusters as 9-connected SBU, **ncb** frameworks can be constructed only from the combination of pyridyl carboxylate–dicarboxylate rather than bipyridyl–dicarboxylate. Further, the node geometry in **ncb** is somewhat distorted on the three

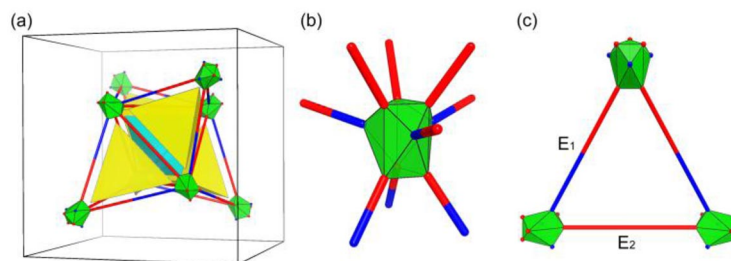


Fig. 8 Topological features of the **ncb** net: (a) The connectivity between the eight nodes in a unit cell. (b) The node with tricapped-trigonal-prism geometry with distortion on the three capped sites. (c) Two kinds of linking fashions, from prism-vertex to capped vertex, and from prism-vertex to prism-vertex between nodes.

capped-vertices from the regular tricapped-trigonal-prism geometry, so that adequate flexibility from the linkers is required to adapt the geometry difference between the node and the cluster.

Combining 4-(pyridin-4-yl)benzoate (pba^-) and naphthalene-2,6-dicarboxylate ($2,6\text{-ndc}^{2-}$) with similar and long lengths, we obtained a highly porous framework $[\text{Ni}^{\text{II}}_2\text{Ni}^{\text{III}}(\mu_3\text{-OH})(\text{pba})_3(2,6\text{-ndc})_{1.5}]_n$ (MCF-19, Fig. 9a), which represented the first example of uninodal 9-connected **ncb** topology [40]. According to the tiling expression of **ncb**, MCF-19 can be considered as a body-centered array of triakis-tetrahedral cages (Fig. 9b). As a consequence, MCF-19 contains a hierarchical porous system consisting of nano-sized **nbo**-type channel surrounded by smaller pores in the triakis-tetrahedral cages (Fig. 9c). The framework collapsing temperature ($250\text{ }^\circ\text{C}$) of MCF-19 is obviously lower than its thermal decomposing temperature ($350\text{ }^\circ\text{C}$), which was attributed to the internal tension caused by the geometry difference between the node and the cluster. Considering that **ncb** has strict requirements to the type and length of ligands, it is worth studying on whether it is possible and how to construct isorecticular porous frameworks based on this prototype.

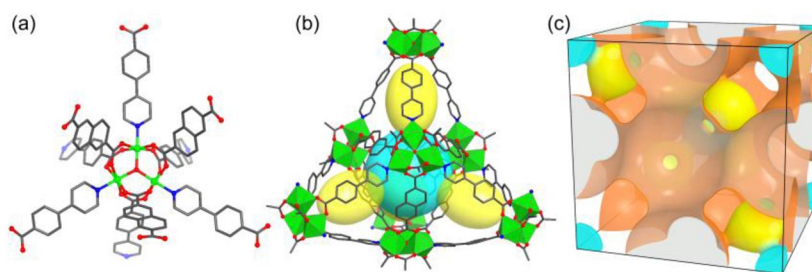


Fig. 9 Structure of MCF-19. (a) The 9-connected $\text{Ni}_3(\mu_3\text{-OH})(\text{RCOO})_6(\text{L}^{\text{B}})_3$ cluster extended by pba^- and $2,6\text{-ndc}^{2-}$ ligands. (b) The triakis-tetrahedral cage. (c) The hierarchical porous system with **nbo**-type channel surrounded by small cavities in the triakis-tetrahedral cages.

To address this question, a geometry analysis method was proposed to figure out the node geometry dependence of the length ratio of the two kinds of edges ($d_r = E_1/E_2$), which indicated an optimal interval of 0.83–1.73 for a better node-geometry compatibility [41]. As shown in Fig. 10, among 5×5 pyridyl–carboxylate–dicarboxylate combinations, 15 were predicted to be promising targets, while other combinations were predicted to be difficult or even impossible, for the **ncb** structure.


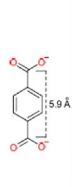
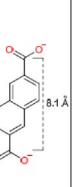
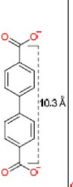
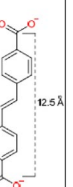
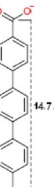
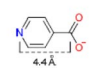
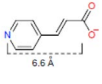
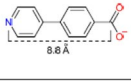
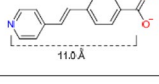
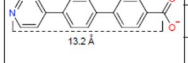
Node	Tricapped trigonal-prism	$E_2/\text{\AA}$	12.3	14.5	16.7	18.9	21.1	
SBU		L^2	a	b	c	d	e	
								
$E_1/\text{\AA}$	L^P		bdc ²⁻	ndc ²⁻	bpdc ²⁻	edba ²⁻	tpdc ²⁻	
11.6	I ina ⁻		d_f	0.94	0.80	0.69	0.61	0.55
			κ^{D^0}	18.4	26.7	37.3	51.7	—
			ϕ^{D^0}	64.3	77.4	92.9	110.1	—
13.8	II pyac ⁻		d_f	1.12	0.95	0.83	0.73	0.65
			κ^{D^0}	11.6	18.0	24.6	32.8	43.2
			ϕ^{D^0}	53.0	63.5	74.1	86.5	100.6
16.0	III pba ⁻		d_f	1.30	1.10	0.96	0.85	0.76
			κ^{D^0}	6.9	12.2	17.5	23.3	30.0
			ϕ^{D^0}	45.2	54.1	62.8	72.1	82.3
18.2	IV pvba ⁻		d_f	1.48	1.26	1.09	0.96	0.86
			κ^{D^0}	3.5	7.8	12.5	17.5	22.7
			ϕ^{D^0}	39.5	46.8	54.6	62.8	71.1
20.4	V pbpa ⁻		d_f	1.66	1.41	1.22	1.08	0.97
			κ^{D^0}	0.9	4.7	8.8	12.8	17.1
			ϕ^{D^0}	35.1	41.5	48.4	55.2	62.1

Fig. 10 Estimating the assemble possibilities of **ncb** net for combinations with different lengths and length ratios of the two kinds of ligands (Reprinted with permission from ref. [41]. Copyright © 2012, Nature Publishing Group).

After systematically screening all the 5×5 combinations, an isorecticular series of **ncb**-type frameworks, $[\text{Ni}^{\text{II}}_2\text{Ni}^{\text{III}}(\mu_3\text{-OH})(\text{L}^P)_3(\text{L}^2)_{1.5}]$ (L^P = pyridylcarboxylate; L^2 = dicarboxylate; Fig. 11), have been successfully discovered, which are 13 cases out of the 15 promising combinations [41]. This ternary prototype has demonstrated a new perspective of isorecticular synthesis with an unprecedented structural diversity and fine-tuned pore metrics by modifying not only the lengths but also the length ratios of the two types of ligands. Without interpenetration, the MCF-19 series has illustrated the systematic adjustment of pore volumes ($0.49\text{--}2.04\text{ cm}^3\text{ g}^{-1}$) and pore sizes ($7.8\text{--}13.0$, $5.2\text{--}12.0$, and $7.4\text{--}17.4\text{ \AA}$), anisotropic modulation of the pore shapes, and modification of not only adsorption capacity but also diffusion kinetics. This study also showed the influence of ligand lengths on thermal stabilities of **ncb** framework. Meanwhile, three other research groups also independently reported the crystal structure of $[\text{Ni}^{\text{II}}_2\text{Ni}^{\text{III}}(\mu_3\text{-OH})(\text{ina})_3(\text{bdc})_{1.5}]$ (MCF-19-Ia, ina^- = isonicotinate) [42–44]. A mixed-metal version of **ncb** framework $[\text{InCo}_2(\mu_3\text{-OH})(\text{ina})_3(\text{bdc})_{1.5}]$ was also reported recently [45].

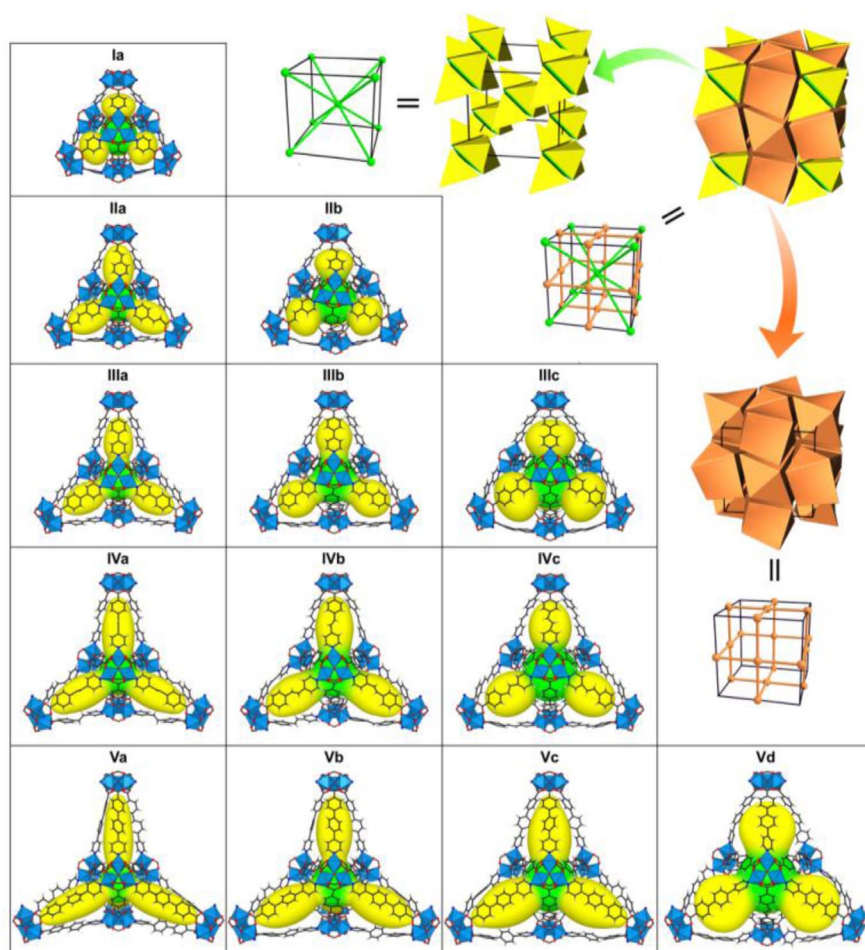


Fig. 11 Isoreticular series of MCF-19. (Reprinted with permission from ref. [41]. Copyright © 2012, Nature Publishing Group).

CONCLUSION

In summary, anisotropic metal–carboxylate–pyridyl clusters obtained by extending the terminal sites of some typical metal–carboxylate clusters expand a new way for the design and synthesis of PCPs with a higher level of complexity and directionality in their self-assembly. Anisotropic building blocks have shown advantages in the discovery of new topologies, multiple-step self-assembly, and anisotropic modification on pore sizes and shapes. Topological isomerism of frameworks has also been encountered in different synthesis conditions. Some anisotropic building blocks also demonstrated strict requirements on ligand functionalities and more complicated geometry principles, which may be solved by simple mathematical calculations.

ACKNOWLEDGMENTS

The authors acknowledge the supporting of the “973 Project” (2012CB821706), NSFC (21121061), and Chinese Ministry of Education (NCET-10-0863 & ROCS).

REFERENCES

1. S. R. Batten, N. R. Champness, X.-M. Chen, J. Garcia-Martinez, S. Kitagawa, L. Öhrström, M. O’Keeffe, M. P. Suh, J. Reedijk. *CrystEngComm* **14**, 3001 (2012).
2. S. Kitagawa, R. Kitaura, S. Noro. *Angew. Chem., Int. Ed.* **43**, 2334 (2004).
3. H. C. Zhou, J. R. Long, O. M. Yaghi. *Chem. Rev.* **112**, 673 (2012).
4. J. P. Zhang, Y. B. Zhang, J. B. Lin, X. M. Chen. *Chem. Rev.* **112**, 1001 (2012).
5. M. O’Keeffe, M. A. Peskov, S. J. Ramsden, O. M. Yaghi. *Acc. Chem. Res.* **41**, 1782 (2008).
6. N. W. Ockwig, O. Delgado-Friedrichs, M. O’Keeffe, O. M. Yaghi. *Acc. Chem. Res.* **38**, 176 (2005).
7. M. Eddaoudi, J. Kim, M. O’Keeffe, O. M. Yaghi. *J. Am. Chem. Soc.* **124**, 376 (2001).
8. H. Li, M. Eddaoudi, M. O’Keeffe, O. M. Yaghi. *Nature* **402**, 276 (1999).
9. A. C. Sudik, A. P. Côté, O. M. Yaghi. *Inorg. Chem.* **44**, 2998 (2005).
10. J. H. Cavka, S. Jakobsen, U. Olsbye, N. Guillou, C. Lamberti, S. Bordiga, K. P. Lillerud. *J. Am. Chem. Soc.* **130**, 13850 (2008).
11. K. Koh, A. G. Wong-Foy, A. J. Matzger. *Angew. Chem., Int. Ed.* **47**, 677 (2008).
12. N. Klein, I. Senkovska, K. Gedrich, U. Stoeck, A. Henschel, U. Mueller, S. Kaskel. *Angew. Chem., Int. Ed.* **48**, 9954 (2009).
13. K. Koh, A. G. Wong-Foy, A. J. Matzger. *J. Am. Chem. Soc.* **131**, 4184 (2009).
14. K. Koh, A. G. Wong-Foy, A. J. Matzger. *J. Am. Chem. Soc.* **132**, 15005 (2010).
15. H. Furukawa, N. Ko, Y. B. Go, N. Aratani, S. B. Choi, E. Choi, A. Ö. Yazaydin, R. Q. Snurr, M. O’Keeffe, J. Kim, O. M. Yaghi. *Science* **329**, 424 (2010).
16. H. Chun. *J. Am. Chem. Soc.* **130**, 800 (2008).
17. H. Chun, H. J. Jung, J. W. Seo. *Inorg. Chem.* **48**, 2043 (2009).
18. H. N. Wang, X. Meng, G. S. Yang, X. L. Wang, K. Z. Shao, Z. M. Su, C. G. Wang. *Chem. Commun.* **47**, 7128 (2011).
19. Z. Ni, A. Yassar, T. Antoun, O. M. Yaghi. *J. Am. Chem. Soc.* **127**, 12752 (2005).
20. J. R. Li, D. J. Timmons, H. C. Zhou. *J. Am. Chem. Soc.* **131**, 6368 (2009).
21. K. Seki, S. Takamizawa, W. Mori. *Chem. Lett.* 332 (2001).
22. K. Seki. *Chem. Commun.* 1496 (2001).
23. D. N. Dybtsev, H. Chun, K. Kim. *Angew. Chem., Int. Ed.* **43**, 5033 (2004).
24. J. Y. Lee, L. Pan, X. Y. Huang, T. J. Emge, J. Li. *Adv. Funct. Mater.* **21**, 993 (2011).
25. B. Q. Ma, K. L. Mulfort, J. T. Hupp. *Inorg. Chem.* **44**, 4912 (2005).
26. H. Chun, D. N. Dybtsev, H. Kim, K. Kim. *Chem.—Eur. J.* **11**, 3521 (2005).
27. Q. Gao, Y. B. Xie, J. R. Li, D. Q. Yuan, A. A. Yakovenko, J. H. Sun, H. C. Zhou. *Cryst. Growth Des.* **12**, 281 (2012).
28. J. P. Zhang, X. C. Huang, X. M. Chen. *Chem. Soc. Rev.* **38**, 2385 (2009).
29. H. Chun, J. Moon. *Inorg. Chem.* **46**, 4371 (2007).
30. M. Kondo, Y. Takashima, J. Seo, S. Kitagawa, S. Furukawa. *CrystEngComm* **12**, 2350 (2010).
31. W. G. Qiu, J. A. Perman, L. Wojtas, M. Eddaoudi, M. J. Zaworotko. *Chem. Commun.* **46**, 8734 (2010).
32. J. A. Perman, A. J. Cairns, L. Wojtas, M. Eddaoudi, M. J. Zaworotko. *CrystEngComm* **13**, 3130 (2011).
33. J. F. Eubank, L. Wojtas, M. R. Hight, T. Bousquet, V. C. Kravtsov, M. Eddaoudi. *J. Am. Chem. Soc.* **133**, 17532 (2011).
34. S. L. Xiang, J. Huang, L. Li, J. Y. Zhang, L. Jiang, X. J. Kuang, C. Y. Su. *Inorg. Chem.* **50**, 1743 (2011).
35. M. H. Zeng, Z. T. Liu, H. H. Zou, H. Liang. *J. Mol. Struct.* **828**, 75 (2007).
36. M. C. Das, H. Xu, S. C. Xiang, Z. J. Zhang, H. D. Arman, G. D. Qian, B. L. Chen. *Chem.—Eur. J.* **17**, 7817 (2011).

37. G. Férey, C. Mellot-Draznieks, C. Serre, F. Millange, J. Dutour, S. Surble, I. Margiolaki. *Science* **309**, 2040 (2005).
38. C. Serre, C. Mellot-Draznieks, S. Surblé, N. Audebrand, Y. Filinchuk, G. Férey. *Science* **315**, 1828 (2007).
39. X. M. Zhang, Y. Z. Zheng, C. R. Li, W. X. Zhang, X. M. Chen. *Cryst. Growth Des.* **7**, 980 (2007).
40. Y. B. Zhang, W. X. Zhang, F. Y. Feng, J. P. Zhang, X. M. Chen. *Angew. Chem., Int. Ed.* **48**, 5287 (2009).
41. Y. B. Zhang, H. L. Zhou, R. B. Lin, C. Zhang, J. B. Lin, J. P. Zhang, X. M. Chen. *Nat. Commun.* **3**, 642 (2012).
42. G. Jiang, T. Wu, S.-T. Zheng, X. Zhao, Q. Lin, X. Bu, P. Feng. *Cryst. Growth Des.* **11**, 3713 (2011).
43. G. J. Ren, S. X. Liu, F. J. Ma, F. Wei, Q. Tang, Y. Yang, D. D. Liang, S. J. Li, Y. G. Chen. *J. Mater. Chem.* **21**, 15909 (2011).
44. E. Yang, Z. S. Liu, S. Lin, S. Y. Chen. *Inorg. Chem. Commun.* **14**, 1588 (2011).
45. S.-T. Zheng, T. Wu, C. Chou, A. Fuhr, P. Feng, X. Bu. *J. Am. Chem. Soc.* **134**, 4517 (2012).